Multiscale Uncertainty Quantification Based on a Generalized Hidden Markov Model

Yan Wang
Assistant Professor
Woodruff School of Mechanical Engineering,
Georgia Institute of Technology,
Atlanta, GA 30332-0405
e-mail: yan.wang@me.gatech.edu

Variability is the inherent randomness in systems, whereas incertitude is due to lack of knowledge. In this paper, a generalized hidden Markov model (GHMM) is proposed to quantify aleatory and epistemic uncertainties simultaneously in multiscale system analysis. The GHMM is based on a new imprecise probability theory that has the form of generalized interval. The new interval probability resembles the precise probability and has a similar calculus structure. The proposed GHMM allows us to quantify cross-scale dependency and information loss between scales. Based on a generalized interval Bayes' rule, three cross-scale information assimilation approaches that incorporate uncertainty propagation are also developed. [DOI: 10.1115/1.4003537]

1 Introduction

Multiscale systems are the ones consisting of hierarchical structures with different sizes and exhibit patterns of behaviors as the diagnostics of interactions among subsystems at lower levels recursively. Human cells, atmospheric turbulence, ecosystems, and product/materials hierarchies are such examples. Among other research issues, uncertainty is an unavoidable artifact of modeling and observation of physical processes and should be assessed in the context of multiscale systems.

The unique challenge in characterizing uncertainty of multiscale systems is how to quantify its propagation across scales accurately and efficiently. Most of the existing stochastic models only focus on one length scale. For multiscale systems, uncertainties propagate between scales and are interdependent. For instance, distributions of defects in crystals determine the reliability of alloy structures. Physical properties of materials are manifestations of atomic-level electron densities and distributions. Therefore, cross-scale correlation should be studied in order to fully understand physical phenomena and support engineering design.

Uncertainty concerns variability and incertitude, which appear universally. The need to quantify variability and incertitude separately has been well recognized [1–3]. Variability is the inherent *randomness* in a system because of fluctuation and perturbation. Variability is also referred to as aleatory uncertainty, stochastic uncertainty, simulation uncertainty, and irreducible uncertainty. In contrast, incertitude is due to lack of perfect knowledge or enough information about the system. It is also known as epistemic uncertainty, reducible uncertainty, and model form uncertainty.

The need of separating aleatory and epistemic uncertainties is more noticeable in multiscale system analysis. Measurement data for very small (e.g., nanoscale physical properties) or very large systems (e.g., global temperature change) are usually scarce, varying greatly in terms of form and quality, or even impossible to be measured. The effect of epistemic uncertainty thus is more evident than in traditional system analysis. The two types of uncertainty need to be represented explicitly if we want to increase the confidence of modeling or simulation results. Neglecting epistemic uncertainty may lead to decisions that are not robust. The typical way to assess robustness is sensitivity analysis [4], which is to check how much variation the analysis result may have if input distribution parameters or types deviate from the ones used in the analysis. Mixing epistemic and aleatory uncertainties may increase the cost of risk management. If extra knowledge or information of the collected data is available, they can be further clustered into smaller groups or intrinsic mathematical relationships can be identified so that variance can be reduced, which reflects pure randomness more accurately for risk analysis.

Therefore, aleatory and epistemic uncertainties need to be quantified simultaneously in multiscale system analysis. In this paper, an imprecise probability approach is proposed to represent the two types of uncertainties. Instead of a precise value of probability $P(E)=p$ associated with an event E, a pair of lower and upper probabilities $P(E)=[\underline{p},\bar{p}]$ is used to include a set of values. The range of the interval $[\underline{p},\bar{p}]$ captures the epistemic uncertainty component. Imprecise probability thus differentiates incertitude from variability both qualitatively and quantitatively, which is an alternative to the traditional sensitivity analysis in probabilistic reasoning.

The interval bounds $\underline{p}$ and $\bar{p}$ can be solicited as the lowest and highest subjective probabilities about a particular event from a domain expert, where probability represents the degree of belief. Different experts may have different beliefs. Even one expert may hesitate to offer just a precise value of probability. In these cases, the range of probabilities gives the interval bounds. Incorporating more beliefs may increase the interval width. When used in data analysis with frequency interpretation, the interval bounds can be confidence intervals that are calculated from data. For instance, the Kolmogorov–Smirnov confidence band to enclose the cumulative distribution function (c.d.f.) can be used, where the width of the band captures epistemic uncertainty because of the lack of information and knowledge. If extra data are collected, the interval width can be reduced, and the confidence band converges toward a precise c.d.f.

The purpose of using imprecise probability in system analysis is to improve the robustness of prediction. The existing sampling-based simulation mechanisms, such as second-order Monte Carlo [5], cannot provide such information efficiently, where a double-loop sampling procedure is used so that the inner loop simulates variability and the outer loop simulates the incertitude associated with models and parameters. There is a need of generic and efficient mathematical framework to study aleatory and epistemic uncertainties in multiscale complex systems. In this paper, we propose a generalized hidden Markov model (GHMM) with a new

Contributed by the Design Automation Committee of ASME for publication in the JOURNAL OF MECHANICAL DESIGN. Manuscript received April 27, 2010; final manuscript received January 23, 2011; published online March 1, 2011. Assoc. Editor: Zissimos P. Mourelatos.

Downloaded 01 Mar 2011 to 130.207.50.192. Redistribution subject to ASME license or copyright; see http://www.asme.org/terms/Terms_Use.cfm

generalized interval probability that is based on generalized interval for multiscale uncertainty quantification. The generalized interval has good algebraic properties, which significantly simplifies the calculus structure of the interval probability.

In the remainder of this paper, overviews of relevant work in multiscale simulation, uncertainty quantification, imprecise probability, and generalized interval are given in Sec. 2. In Sec. 3, the new imprecise probability theory based on the generalized intervals is described. In Sec. 4, the GHMM is proposed. Three cross-scale information assimilation approaches are developed and demonstrated in Sec. 5.

2 Background

2.1 Stochastic Models to Simulate With Variability. Various stochastic models to accommodate variability have been developed at different scales. At the traditional macro- or bulk-scale of engineering, stochastic or probabilistic finite element analysis with random fields has been extensively studied. The basic idea is to incorporate variabilities of geometry, material properties, and loads in finite element analysis (FEA) [6]. Analysis methods of numerical approximations [7], spectral approximations by the Karhunen–Loève (KL) decomposition [8], as well as its generalizations [9–11], and optimization [12] have been developed.

At the mesoscale, dislocation dynamics [13] is a popular tool to simulate plastic deformation of crystalline structures. Extended from deterministic models, stochasticity was introduced into dislocation dynamics simulation to incorporate the fluctuation effects of internal stress [14] and spatial distributions [15,16] caused by long-range dislocation interaction and thermal dissipation [17] during plastic flow.

The models reviewed above only consider variability within one scale. Assumptions are made such that randomness at macroscale is independent of that at microscale. This homogenization approach does not always model the real world. For example, the effective variance of moduli obtained by averaging over small domains of composite materials does not agree with the one obtained from a sufficiently large representative volume element. Furthermore, damage and fracture are highly sensitive to very local defects [18]. Decoupling variational information between length scales will compromise the accuracy of predictions.

2.2 Multiscale Simulation With Variability. Plenty of research has been done on deterministic multiscale simulation, while relatively little research is focused on stochastic information integration. Recently, Choi et al. [19] represented variabilities as multiscale Gaussian models with a pyramid graph structure. Multiscale information assimilation was achieved by a so-called walk-sum analysis for both long-range and local dependencies. As an extension of Arlequin coupling framework, Chamoin et al. [20] proposed a stochastic coupling approach based on homogenization of material properties between length scales for Monte Carlo simulation. Ganapathysubramanian and Zabaras [21] developed an upscaling approach to derive coarse-scale probability distributions from fine-scale distributions based on sampling in low-dimensional space. Arnst and Ghanem [22] took another upscaling approach to approximate fine-scale probability distributions by the KL decomposition. Chen and co-workers [23,24] also developed an upscaling approach based on the KL decomposition and integrated it with stochastic FEA.

The above methods are intended to solve the issue of multiscale variability information exchange. Domain specific assumptions of probability distributions were made so that analysis is computationally tractable. More importantly, aleatory and epistemic uncertainties were not differentiated. Consequently, the effects of lack of information versus fluctuation are indistinguishable. Given the very different nature of variability and incertitude, independent quantification of the two is useful to understand the analysis results and make appropriate decisions accordingly. The GHMM proposed here is generic enough to support both parametric and nonparametric probabilistic modeling without the assumption of distributions, at the same time differentiating aleatory and epistemic uncertainties with imprecise probability.

2.3 Imprecise Probability. Probability theory provides common ground to quantify uncertainty and so far is the most popular approach. Uncertainties are quantified by precise values of probability measures and their parameters (e.g., means and higher-order moments). However, precise probability theory has limitations in representing epistemic uncertainty. The most significant one is that it does not differentiate *total ignorance* from other probability distributions. Total ignorance means that the analyst has zero knowledge about the system under study. Based on the principle of maximum entropy, uniform distributions are usually assumed when traditional probability theory is applied in this case. A problem arises because introducing a uniform or any particular form of distribution has itself introduced extra information that is not justifiable by the zero knowledge. The commonly used uniform distribution where all possible values are equally likely is not guaranteed to be true because we are totally ignorant. This leads to the Bertrand-style paradoxes such as the van Fraassen's cube factory [25]. "Knowing the unknown" does not represent the total ignorance. In imprecise probability $P=[0,1]$ accurately represents the total ignorance.

Another limitation of precise probability is representing *indeterminacy* and *inconsistency* in the context of subjective probability. When no data are available and people have limited ability to determine the precise values of their own subjective probabilities, precise probability does not capture indeterminacy. When subjective probabilities from different people are inconsistent, it does not capture a range of opinions or estimations adequately without assuming some consensus of precise values on the distribution of opinions. "Agreeing the disagreed" is not the best way to capture inconsistency.

Imprecise probability $[\underline{p},\bar{p}]$ combines epistemic uncertainty (as an interval) with aleatory uncertainty (as probability measure), which is regarded as a generalization of traditional probability. Gaining more knowledge can reduce the level of imprecision and indeterminacy, i.e., the interval width. When $\underline{p}=\bar{p}$, the degenerated interval probability becomes a traditional precise one. Our proposed approach uses imprecise probabilities to quantify aleatory and epistemic uncertainties simultaneously. Many forms of imprecise probabilities have been developed. For example, the Dempster–Shafer evidence theory [26,27] characterizes evidence with discrete probability masses associated with a power set of values. The behavioral imprecise probability theory [1,28] models uncertainties with the lower and upper previsions following the notations of de Finetti's subjective probability theory. The possibility theory [29] represents uncertainties with necessity-possibility pairs. Probability bound analysis [30] captures uncertain information with pairs of lower and upper distribution functions or p-boxes. F-probability [31] represents an interval probability as a set of probabilities with the Kolmogorov properties. A random set [32] is a multivalued mapping from the probability space to the value space. Interval probability [33] computes imprecision with interval analysis. Fuzzy probability [34] considers probability distributions with fuzzy parameters. A cloud [35] is a combination of fuzzy sets, intervals, and probability distributions.

One common problem of the above set-based imprecise probability theories is that the calculation is cumbersome. Linear and nonlinear optimization methods are depended on to search lower and upper bounds of probabilities during reasoning. Different from them, we recently proposed an imprecise probability with a generalized interval form [36,37], where the calculus structure is greatly simplified based on the algebraic properties of the Kaucher arithmetic [38] for the generalized interval.

2.4 Generalized Interval. Generalized interval [39,40] is an extension of the set-based classical interval [41] with better alge-

Downloaded 01 Mar 2011 to 130.207.50.192. Redistribution subject to ASME license or copyright; see http://www.asme.org/terms/Terms_Use.cfm

braic and semantic properties based on the Kaucher arithmetic [38]. A generalized interval $\mathbf{x} := [\underline{x}, \overline{x}] (\underline{x}, \overline{x} \in \mathbb{R})$ is not constrained by $\underline{x} \leq \overline{x}$ anymore. Therefore, [0.2,0.1] is also a valid interval and called *improper*, while the traditional interval [0.1,0.2] is called *proper*. Based on the theorems of interpretability [39], a generalized interval provides more semantic power to help verify completeness and soundness of range estimations by logic interpretations. A complete range estimation of possible values includes all possible occurrences. A sound range estimation does not include impossible occurrences. More information of generalized interval can be found in Refs. [42–44].

Compared with the *semigroup* formed by the classical set-based intervals, generalized intervals form a *group*. This property significantly simplifies the computational structure. The set of generalized intervals is denoted by $\mathbb{KR} = \{[\underline{x}, \overline{x}] | \underline{x}, \overline{x} \in \mathbb{R}\}$. The set of proper intervals is $\mathbb{IR} = \{[\underline{x}, \overline{x}] | \underline{x} \leq \overline{x}\}$, and the set of improper interval is $\overline{\mathbb{IR}} = \{[\underline{x}, \overline{x}] | \underline{x} \geq \overline{x}\}$. The relationship between proper and improper intervals is established with the operator *dual* as

$$\text{dual}[\underline{x}, \overline{x}] := [\overline{x}, \underline{x}] \tag{2.1}$$

The *less than or equal to* partial order relationship between two generalized intervals is defined as

$$[\underline{x}, \overline{x}] \leq [\underline{y}, \overline{y}] \Leftrightarrow \underline{x} \leq \underline{y} \wedge \overline{x} \leq \overline{y} \tag{2.2}$$

Based on the generalized interval, the new form of imprecise probability resembles the classical precise probability.

3 Generalized Interval Probability

DEFINITION 1. Given a sample space Ω and a σ-algebra $\mathcal{A}$ of random events over Ω, the *generalized interval probability* $\mathbf{p} \in \mathbb{KR}$ is defined as $\mathbf{p}: \mathcal{A} \rightarrow [0,1] \times [0,1]$, which obeys the axioms of Kolmogorov: (1) $\mathbf{p}(\Omega) = [1,1]$, (2) $[0,0] \leq \mathbf{p}(E) \leq [1,1] (\forall E \in \mathrm{A})$, and (3) for any countable mutually disjoint events $E_i \cap E_j = \emptyset (i \neq j)$, $\mathbf{p}(\cup_{i=1}^{n} E_i) = \Sigma_{i=1}^{n} \mathbf{p}(E_i)$. Here "$\leq$" is defined in Eq. (2.2).

DEFINITION 2. The probability of *union* is defined as $\mathbf{p}(A) := \Sigma_{S \subseteq A} (-\text{dual})^{|A|-|S|} \mathrm{p}(S)$ for $A \subseteq \Omega$.

The most important property of the generalized interval probability is the *logic coherence constraint* (LCC): for a mutually disjoint event partition $\cup_{i=1}^{n} E_i = \Omega$, $\Sigma_{i=1}^{n} \mathbf{p}(E_i) = 1$. The LCC ensures that the generalized interval probability is logically coherent with the precise probability. For instance, given that $\mathbf{p}(\text{down}) = [0.2, 0.3]$, $\mathbf{p}(\text{idle}) = [0.3, 0.5]$, and $\mathbf{p}(\text{working}) = [0.5, 0.2]$ for a system's working status, we can interpret it as

$$(\forall p_1 \in [0.2,0.3])(\forall p_2 \in [0.3,0.5])(\exists p_3 \in [0.2,0.5])(p_1 + p_2 + p_3 = 1)$$

Accordingly, we differentiate nonfocal events (*working* in this example) from focal events (*down* and *idle*). An event E is *focal* if the associated semantics for $\mathbf{p}(E)$ is universal ($\forall$). Otherwise, it is *nonfocal* if the associated semantics is existential ($\exists$). While the epistemic uncertainty associated with a focal event is critical to the analyst, the one associated with a nonfocal event is not.

The concepts of conditional probability and independence are essential for the classical probability theory. With them, we can decompose a complex problem into simpler and more manageable components. Similarly, they are critical for imprecise probabilities. Different from all other forms of imprecise probabilities, which are based on convex probability sets, our conditional probability is defined directly from marginal probability.

DEFINITION 3. If $\mathbf{p}(C) > 0$, the *conditional probability* $\mathbf{p}(E|C)$ for all $E, C \in \mathcal{A}$ is defined as

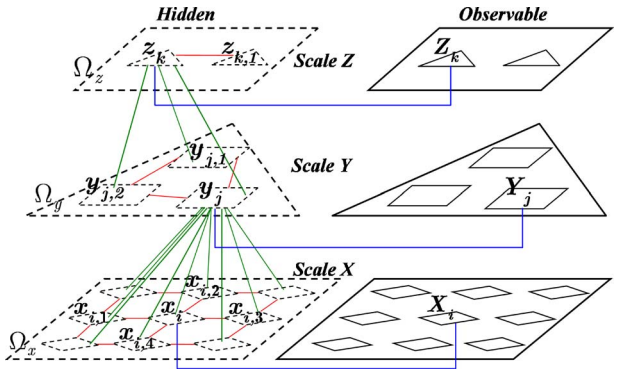

Fig. 1 The generalized hidden Markov model for multiscale systems to capture spatial and scale dependency

$$\mathbf{p}(E|C) := \frac{\mathbf{p}(E \cap C)}{\text{dual}\mathbf{p}(C)} = \left[\frac{\underline{p}(E \cap C)}{\underline{p}(C)}, \frac{\overline{p}(E \cap C)}{\overline{p}(C)} \right] \tag{3.1}$$

Thanks to the unique algebraic properties of generalized intervals, this definition can greatly simplify computation in applications. Only algebraic computation is necessary.

DEFINITION 4. For $A, B, C \in \mathcal{A}$, A and B are said to be *conditionally independent* given C if and only if

$$\mathbf{p}(A \cap B|C) = \mathbf{p}(A|C)\mathbf{p}(B|C) \tag{3.2}$$

DEFINITION 5. For $A, B \in \mathcal{A}$, $\mathcal{A}$ and B are said to be *independent* if and only if

$$\mathbf{p}(A \cap B) = \mathbf{p}(A)\mathbf{p}(B) \tag{3.3}$$

The independence in Definition 5 is a special case of conditional independence in Definition 4, where C is the complete sample space Ω. The conditional independence in Eq. (3.2) can also have a second form, as shown in Theorem 3.1. The proofs of all theorems are included in the Appendixes A and F.

THEOREM 3.1. $\mathbf{p}(A \cap B|C) = \mathbf{p}(A|C)\mathbf{p}(B|C) \Leftrightarrow \mathbf{p}(A|B \cap C) = \mathbf{p}(A|C)$.

4 Generalized Hidden Markov Model (GHMM)

We propose a new and generic probabilistic model to account for aleatory and epistemic uncertainties in complex systems. The proposed GHMM essentially captures spatial dependency. Figure 1 is an illustration of GHMM for multiscale systems, where the spatial domains in three length scales Ω_x, Ω_y, and Ω_z are subdivided into cells. The state of each cell is represented as a random variable, denoted as x_i, y_j, z_k, respectively, at three scales. If the state value of a cell is dependent on those values of neighboring cells, the dependencies or correlations are denoted by the connections between cells in the graphical model.

The spatial dependency or correlation relationships are expressed as conditional probabilities. For instance, $\mathbf{p}(x_i = a | x_{i,1} = b_1, x_{i,2} = b_2, \ldots, x_{i,l} = b_l)$ is the probability that the state variable x_i has value of a given that its l neighboring cells have the respective state values of $(b_1, \ldots, b_l)$. In the example of Fig. 1, x_i has $l = 4$ neighbors. Notice that neighbors do not necessarily mean that they are spatially close. If long-range couplings exist, one cell could be dependent on or correlated with another even when they are spatially far apart.

Between different scales, there are also dependency relationships. The scale dependency is also represented as a conditional probability. For instance, in Fig. 1, the state of cell y_j at scale Y is dependent on the state values of the corresponding subdomain Ω_x, i.e., $\mathbf{p}(y_j | x_1, \ldots, x_i, \ldots, x_9)$.

In general, the true state values of cells may or may not be directly observable. Theoretically, all observed values in experiments contain the effects of aleatory and epistemic uncertainties.

Downloaded 01 Mar 2011 to 130.207.50.192. Redistribution subject to ASME license or copyright; see http://www.asme.org/terms/Terms_Use.cfm

Therefore, the observed states are just another set of random variables that are dependent on true state values. Here, the observation dependency is included in the GHMM. Without loss of generality, we assume that each of the cells in different scales has its corresponding observable state. For instance, in Fig. 1, the true states of the cells on the left-hand side are hidden, and the corresponding observations are on the right-hand side. The probability of observing $X_i=b$ given that $x_i=a$ is $\mathbf{p}(X_i=b|x_i=a)$. Similarly, we have $\mathbf{p}(Y_j|y_j)$ and $\mathbf{p}(Z_k|z_k)$ at other length scales. If there are states that are not observable, the number of observation dependency relationships is reduced.

The proposed GHMM is a generalization of hidden Markov models (HMMs) [45,46] to analyze systems under both aleatory and epistemic uncertainties. Even though there has been some research to extend HMM to hierarchical models and apply them to pattern recognition such as natural language [47] and image classifications [48,49], epistemic uncertainty is not explicitly captured in these Markov models. The most important and unique generalization of the proposed GHMM is that imprecise probabilities based on generalized intervals are used in the model. With imprecise probabilities, both types of uncertainties can be explicitly incorporated. With generalized intervals, inference and reasoning can be significantly simplified. Therefore, the proposed model improves computational efficiency while gaining more information from analysis results. Notice that the model illustrated in Fig. 1 shows spatial dependency only. To capture temporal dependency, state transitions can also be achieved. That is, a GHMM with one-dimensional neighborhood relationships will represent state transition history within one cell in Fig. 1.

We call the GHMM *generalized* because of three levels of generalizations. First, our multiscale Markov model is a generalization of commonly used Markov chains and hidden Markov models. Second, our Markov model with imprecise probabilities is a generalization of traditional models with precise probabilities. Third, our new form of imprecise probability based on generalized intervals is also a generalization of interval probabilities. The GHMM is generally applicable to various uncertainty quantification problems. In this paper, we apply it in multiscale system design and analysis.

With the incorporation of generalized interval probability, a concise form of GHMM properties similar to the traditional precise probability can be achieved. The most important properties are *localities*. These include the locality of observation and the locality of scale.

THEOREM 4.1 (locality of observation). *For two disjoint subdomains $\mathcal{A}_i$ and $\mathcal{A}_j$ at scale X*, if the hidden states $x_{i\in\mathcal{A}_i}$ *and* $x_{j\in\mathcal{A}_j}$ *are independent and the corresponding observations are also independent, then*

$$\mathbf{p}(X_{\mathcal{A}_i},X_{\mathcal{A}_j}|x_{i\in\mathcal{A}_i},x_{j\in\mathcal{A}_j})=\mathbf{p}(X_{\mathcal{A}_i}|x_{i\in\mathcal{A}_i})\mathbf{p}(X_{\mathcal{A}_j}|x_{j\in\mathcal{A}_j})$$

Theorem 4.1 provides the algebraic convenience to decompose a complex system into smaller subsystems within one scale. Independent experimental measurements can be performed without losing the grand picture of aleatory and epistemic uncertainties of the whole system.

THEOREM 4.2 (locality of scale). *If $\mathcal{A}_i$, $\mathcal{B}_j$, and $\mathcal{C}_k$ are subdomains at scales X, Y, and Z*, respectively, with $\mathcal{A}_i\subset\mathcal{B}_j\subset\mathcal{C}_k$, then

$$\mathbf{p}(x_{\mathcal{A}_i}|y_{\mathcal{B}_j},z_{\mathcal{C}_k})=\mathbf{p}(x_{\mathcal{A}_i}|y_{\mathcal{B}_j}) \quad \text{and} \quad \mathbf{p}(z_{\mathcal{C}_k}|y_{\mathcal{B}_j},x_{\mathcal{A}_i})=\mathbf{p}(z_{\mathcal{C}_k}|y_{\mathcal{B}_j})$$

Theorem 4.2 allows us to simplify the analysis with multiple scales. The propagation of uncertain information between scales is only limited to the two that are adjacent or closely related. It also indicates that the information exchange in the GHMM is in both top-down and bottom-up directions. For instance, in a polycrystalline piezoelectric ceramic material, the variation of lattice distortion for individual unit cells is correlated with the polarization of the grain which the cells belong to. Given that the dependency between lattice-level and grain-level uncertainties has been considered, the variation of lattice-level local distortion can be regarded as being independent of the overall anisotropic electromechanical properties of the whole piezoelectric disk because the macroscopic properties of the polycrystalline solid are the homogenization of all grains, whereas those of each grain in turn are the manifestation of average structural properties from all cells within it.

The simplicity of the scale and observation localities is due to the definition of conditional probability in Eq. (3.1) as well as the group properties of the generalized interval.

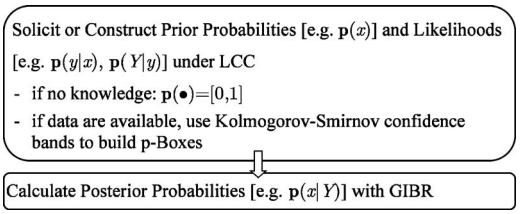

Fig. 2 The illustration of cross-scale information assimilation based on GIBR

5 Cross-Scale Information Assimilation

When small-scale (or large-scale) experiments are not possible, or the measurements are not feasible or dependable at one particular scale, we may conduct experiments at a larger (or smaller) scale to measure system properties so that information can be combined to validate models or assumptions. For instance, in design of new devices using nanomaterials, instead of directly measuring atomic-level properties, which is usually expensive or even impossible, the measurement of aggregated properties at macroscale can be easier and more accurate. In contrast, it is impossible to measure global temperature change. We only depend on regional ocean water temperature changes to predict the global picture. Cross-scale information assimilation thus is an important tool in studying multiscale systems, which is based on a *generalized interval Bayes' rule* (GIBR).

THEOREM 5.1 (GIBR). *The generalized interval Bayes' rule states that*

$$\mathbf{p}(E_i|A)=\frac{\mathbf{p}(A|E_i)\mathbf{p}(E_i)}{\sum_{j=1}^{n}\text{dual }\mathbf{p}(A|E_j)\text{dual }\mathbf{p}(E_j)} \tag{5.1}$$

where $E_i(i=1,\ldots,n)$ are mutually disjoint event partitions of Ω and $\Sigma_{j=1}^{n}\mathbf{p}(E_j)=1$.

Based on the GIBR, the problem of cross-scale information assimilation under aleatory and epistemic uncertainties can be formulated in several ways, including single-point observation, multipoint observation, and multipoint multiscale observation. The general process of cross-scale information assimilation based on the GIBR is illustrated in Fig. 2. Prior probabilities and likelihoods are constructed or solicited. If data are available, we may use the Kolmogorov–Smirnov confidence bands as p-boxes and calculate interval probabilities. If no data are available, domain experts may give estimates of interval probabilities. In either case, the logic coherence constraint in Sec. 3 should be satisfied. If no knowledge is available at all, $\mathbf{p}=[0,1]$ should be used.

5.1 Single-Point Observation. The simplest cross-scale assimilation is by the single-point observation. This approach allows that the uncertainty estimation at one scale is used to either validate the model prediction or update the information at a different scale. Suppose that the states of one or more variables $x_1,\ldots,x_l$ at scale X are not directly observable, and the system can be observed via the variable Y corresponding to the unobservable y at scale Y instead. Then the estimation is calculated as follows.

Downloaded 01 Mar 2011 to 130.207.50.192. Redistribution subject to ASME license or copyright; see http://www.asme.org/terms/Terms_Use.cfm

THEOREM 5.2. *Given* $\mathbf{p}(y|x_1,\ldots,x_L)$ *for variables* $x_1,\ldots,x_L$ *at scale X and y at scale Y,* $\mathbf{p}(Y|y)$ *for observable Y corresponding to y , and the prior estimate* $\mathbf{p}(x_1,\ldots,x_L)$*, the posterior imprecise probability* $\mathbf{p}(x_1,\ldots,x_L|Y)$ *is obtained as*

$$\mathbf{p}(x_1,\ldots,x_L|Y)=\frac{\mathbf{p}(x_1,\ldots,x_L)\int \mathbf{p}(Y|y)\mathbf{p}(y|x_1,\ldots,x_L)dy}{\text{dual}\int\cdots\iint \mathbf{p}(Y|y)\mathbf{p}(y|x_1,\ldots,x_L)\mathbf{p}(x_1,\ldots,x_L)dydx_1\cdots dx_L}$$

5.2 An Example of Single-Point Observation. Carbon nanotubes (CNTs) have unique electrical and mechanical properties, and CNT polymer composites have been applied in various designs of sensors and actuators. In design of biomimetic actuators based on ionic polymer composite, the incorporation of CNT in polymer matrix can improve the electromechanical property. In the design of Deshmukh and Ounaies [50] as shown in Fig. 3, significant forces can be generated with CNTs when low dc voltages are applied on the polymer composite actuators. The amount of CNT, the conductivity of polymer composites, and the level of induced strain are correlated.

Designer may want to know whether the electrical conductivity of the nanotube itself in composites meets the specification, and experimental studies are needed. Instead of directly measuring the resistivity of individual CNTs with diameters of about 10 nm, we can measure those from CNT composites with the sizes of 1 μm or more, which is much easier and more accurate. The electrical conductivity of CNTs is sensitively dependent on the geometry of tubes, particularly diameter and helicity. Because of the variation of geometry and defects during the fabrication process, the measured quantities are stochastic in nature. At the same time, epistemic uncertainty is associated with measurement because of the lack of data, inconsistent observations, and measurement errors.

Relatively limited data are available for direct measurement of individual CNTs' resistivity. Table 1 lists two sets of samples that published in Refs. [51,52]. Notice that the first paper as shown in the left column reported measurement errors or uncertainty with the ± ranges. The second paper used a different form and did not record ranges. Yet the first and fifth samples are right censored and recorded with "≥." The imprecise and incomplete information is the source of epistemic uncertainty. Both of the sample sizes (6 and 8) are small. It is obvious that these two sets of data are inconsistent, which also shows the importance of imprecise probability in such applications.

We can use observations of CNT composite conductivity at mesoscale to assess the individual CNT's resistivity at nanoscale. First, we construct prior probabilities of individual CNT's resistivity. For simplicity, only the data in the first column of Table 1 are used. The empirical c.d.f. for each of the lower, middle, and upper observations are solid lines in Fig. 4. If a parametric distribution is required, we can fit the data by the lognormal distribution, plotted as dotted curves in Fig. 4, for three sets of data (lower bound, middle, and upper bound) in terms of maximum likelihood. However, given the very limited number of samples, the parametric models are not plausible. We would rather use a nonparametric model with the empirical c.d.f.'s without the assumption of the distribution type. Therefore, the empirical interval c.d.f. or p-box is constructed based on the Kolmogorov–Smirnov confidence band [30]. The 95% confidence lower and upper limits from the middle observation (red line) are shown as the blue and green dashed lines, respectively, in Fig. 4. They are calculated by

Table 1 Resistivity measurements of individual CNTs

Resistivity [51] (Ω m)	Resistivity [52] (Ω m)
$\rho \pm \delta$ -6 samples	ρ -8 samples
19.5 ± 2.0	≥80
7.8 ± 1.0	0.012
46.0 ± 1.8	0.0075
37.6 ± 1.0	580
48.9 ± 4.3	≥0.4
117 ± 19	0.00051
	0.098
	0.020

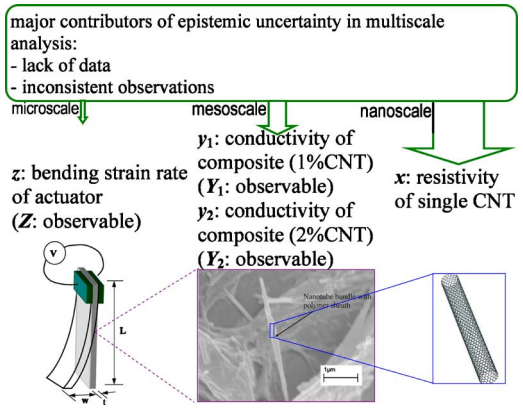

Fig. 3 CNT composites in design of biomimetic actuator [50]

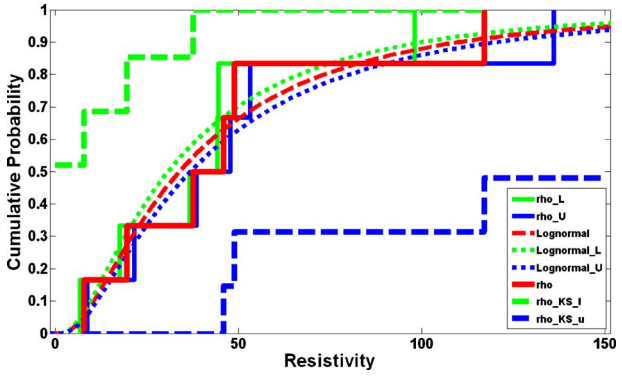

Fig. 4 Empirical c.d.f.'s and the distributions of data from Ref. [51]

Downloaded 01 Mar 2011 to 130.207.50.192. Redistribution subject to ASME license or copyright; see http://www.asme.org/terms/Terms_Use.cfm

Table 2 Conductivity measurements of CNT polymer composites with CNT concentration of 1.0 wt %

Maximum conductivity σ (Ω m^{-1})	No. of samples
1.0×10^{-4}	1
1.0×10^{-3}	1
5.0×10^{-3}	1
2.0×10^{-2}	2
1.0×10^{-1}	3
2.0×10^{-1}	1
3.0×10^{-1}	1
4.0×10^{-1}	1
2.0	1
5.0	1
1.0×10^{1}	2
5.0×10^{1}	1
1.0×10^{2}	1

$\min(1,\max(0,\rho\pm D_{\alpha,n}))$, where $D_{\alpha,n}$ depends on the sample size n and confidence level α. Here, $n=6$, $\alpha=0.025$, and $D_{0.025,6}=0.51926$. This confidence band ensures that the probability of the unknown distribution function being within the band is at least 95%.

With the p-box formed by the Kolmogorov–Smirnov confidence band and the Dempster–Shafer's structure of basic probability assignment (BPA) $m:2^{A}\rightarrow[0,1]$, we can determine the lower and upper probabilities of the resistivity. Specifically, the p-box is viewed as a stack of rectangles. The width of each rectangle is the focal element that defines the interval range of a BPA, whereas the height of the rectangle is the value of the BPA. The BPAs are $m(0\le\rho<46.0)=3/6-D_{0.025,6}=0.1474$, $m(0\le\rho<48.9)=1/6$, $m(0\le\rho<117)=1/6$, $m(0\le\rho<\infty)=D_{0.025,6}-(1-D_{0.025,6})=0.0385$, $m(7.8\le\rho<\infty)=1/6$, $m(19.5\le\rho<\infty)=1/6$, and $m(37.6\le\rho<\infty)=1-2/6-D_{0.025,6}=0.1474$.

Based on the Dempster–Shafer's belief function

$$\underline{p}(A)=\sum_{i:A_i\subseteq A}m(A_i) \tag{5.2}$$

and plausibility function

$$\bar{p}(A)=\sum_{i:A_i\cap A\neq\varnothing}m(A_i) \tag{5.3}$$

we can find the lower and upper probabilities. For instance, the lower and upper probabilities that the individual CNT resistivity are less than 50 Ω m are $\underline{p}(\rho<50)=m(0\le\rho<46.0)+m(0\le\rho<48.9)=0.3140$ and $\bar{p}(\rho<50)=1$, respectively. Thus the prior probability is $\mathbf{p}(x)=[0.3140,1]$.

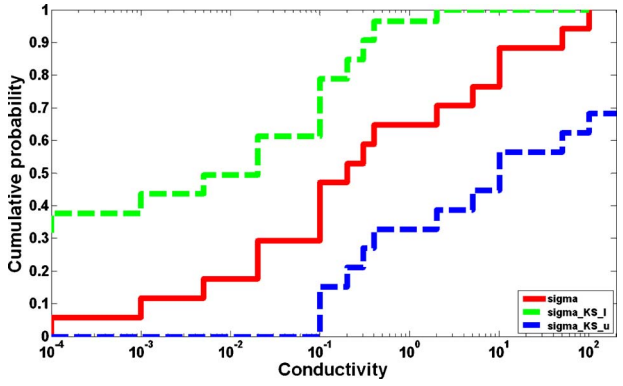

Fig. 5 Empirical c.d.f. of composites conductivity with 1.0 wt % of CNT from Ref. [53]

Compared with individual CNT measurement, the measurement for CNT polymer composites is much easier to achieve. More than 200 publications have reported on the electrical properties of CNT polymer composites. Bauhofer and Kovacs [53] recently summarized those experimental results. The conductivity of composites with CNT concentration 1.0 wt % is compiled and listed in Table 2. The empirical c.d.f. is plotted in Fig. 5 as the red line. Similarly, the 95% Kolmogorov–Smirnov confidence limits (dash lines) are calculated as lower and upper probability bounds.

Similarly, the lower and upper probabilities can be determined based on Eqs. (5.2) and (5.3). For instance, we have

$$\mathbf{p}(\text{conductivity with } 1\%\text{CNT}<0.1|\rho<50)=p(y_1|x)=[0.1526,0.6121]$$

which is the probability that the CNT composite conductivity is less than 0.1 Ω m^{-1} given that the resistivity of the used individual CNTs is less than 50 Ω m.

No information is available for the composite conductivity if the individual CNT resistivity used is greater than 50 Ω m. That is, $\mathbf{p}(y_1|x^C)=[0,1]$, and it represents the total ignorance. In addition, $\mathbf{p}(x^C)=1-\text{dual}\mathbf{p}(x)=[0.6860,0]$, $\mathbf{p}(y_1^C|x)=1-\text{dual}\mathbf{p}(y_1|x)=[0.8474,0.3879]$, and $\mathbf{p}(y_1^C|x^C)=1-\text{dual}\mathbf{p}(y_1|x^C)=[1,0]$. Further, we can reasonably assume the measurement of composite conductivity is fairly reliable with $\mathbf{p}(Y_1|y_1)=[0.8,0.9]$ and $\mathbf{p}(Y_1^C|y_1^C)=[0.8,0.9]$. Thus, $\mathbf{p}(Y_1^C|y_1)=[0.2,0.1]$ and $\mathbf{p}(Y_1|y_1^C)=[0.2,0.1]$.

If an additional observation of Y_1 (conductivity <0.1) is obtained, then based on Theorem 5.2 we can assert that

$$\mathbf{p}(x|Y_1)=\frac{\mathbf{p}(x)[\mathbf{p}(Y_1|y_1)\mathbf{p}(y_1|x)+\mathbf{p}(Y_1|y_1^C)\mathbf{p}(y_1^C|x)]}{\text{dual}\begin{bmatrix}\mathbf{p}(Y_1|y_1)\mathbf{p}(y_1|x)\mathbf{p}(x)\\+\mathbf{p}(Y_1|y_1)\mathbf{p}(y_1|x^C)\mathbf{p}(x^C)\\+\mathbf{p}(Y_1|y_1^C)\mathbf{p}(y_1^C|x)\mathbf{p}(x)\\+\mathbf{p}(Y_1|y_1^C)\mathbf{p}(y_1^C|x^C)\mathbf{p}(x^C)\end{bmatrix}}=[0.4002,1]$$

This posterior probability shows that the epistemic uncertainty level of individual CNT property is reduced to $1-0.4002=0.5998$ from the prior estimate of $1-0.3140=0.6860$.

Notice that interval probability allows us to calculate posterior probabilities even when no data are available. When the total ignorance of $\mathbf{p}=[0,1]$ is applied, there is no risk of assuming certain prior probabilities. In addition, the calculation of interval posterior probabilities based on our generalized interval probability has a much simpler form than other forms of imprecise probabilities.

In summary, the example in this section demonstrates that the observation or measurement at one scale can be used to update and assess uncertainties of a relevant quantity at a different scale. Notice that all random variables with imprecise probabilities include both aleatory and epistemic uncertainties. This process is

Table 3 Conductivity measurements of CNT polymer composites with CNT concentration of 2.0 wt %

Maximum conductivity σ (Ω m^{-1})	No. of samples
3.0×10^{-6}	1
1.0×10^{-4}	1
1.0×10^{-3}	1
1.0×10^{-2}	2
3.0×10^{-2}	1
4.0×10^{-2}	1
5.0×10^{-2}	2
1.0×10^{-1}	2
1.0	1

Downloaded 01 Mar 2011 to 130.207.50.192. Redistribution subject to ASME license or copyright; see http://www.asme.org/terms/Terms_Use.cfm

also useful to validate models or hypotheses concerned with quantities that are difficult or costly to measure if intrinsic dependencies between quantities of two scales exist.

5.3 Multipoint Observation. If there are multiple points of observation $Y_1,\ldots,Y_M$ available instead of just one, the estimates of $x_1,\ldots,x_L$ may be more accurate.

THEOREM 5.3. *Given* $\mathbf{p}(y_1,\ldots,y_M|x_1,\ldots,x_L)$ *for variables* $x_1,\ldots,x_L$ *at scale* X *and* $y_1,\ldots,y_M$ *at scale* Y, $\mathbf{p}(Y_1,\ldots,Y_M|y_1,\ldots,y_M)$ *for observable* Y_m *corresponding to* y_m $(m=1,\ldots,M)$, *and the prior estimate* $\mathbf{p}(x_1,\ldots,x_L)$, *the posterior imprecise probability* $\mathbf{p}(x_1,\ldots,x_L|Y_1,\ldots,Y_M)$ *is obtained as*

$$\mathbf{p}(x_1,\ldots,x_L|Y_1,\ldots,Y_M)=\frac{\mathbf{p}(x_1,\ldots,x_L)\int\cdots\int\left[\begin{array}{l}\prod_{m=1}^{M}\mathbf{p}(Y_m|y_m)\\ \times\prod_{m=1}^{M}\mathbf{p}(y_m|x_1,\ldots,x_L)\end{array}\right]dy_1\cdots dy_M}{\text{dual}\int\cdots\int\left[\begin{array}{l}\prod_{m=1}^{M}\mathbf{p}(Y_m|y_m)\\ \times\prod_{m=1}^{M}\mathbf{p}(y_m|x_1,\ldots,x_L)\\ \times\mathbf{p}(x_1,\ldots,x_L)\end{array}\right]dy_1\cdots dy_M dx_1\cdots dx_L}$$

5.4 An Example of Multipoint Observation. We still use the CNT composite example in Sec. 5.2 to illustrate. The conductivity of the composite material is correlated with the concentration of CNT or the ratio of weights between CNT and polymer. The general trend for low concentrations is that more CNT leads to higher conductivity. Therefore, if the conductivities of two composites with different CNT concentrations, e.g., 1.0% and 2.0%, are measured as Y_1 and Y_2, respectively, the estimate $\mathbf{p}(x)$ can be updated based on Theorem 5.3.

From the data in Ref. [53], the conductivity of composite with CNT concentration 2.0% is compiled and listed in Table 3. Similarly,

$$\mathbf{p}(\text{conductivity with } 2\%\text{CNT}<0.1|\rho<50)=\mathbf{p}(y_2|x)=[0.5412,1]$$

is calculated based on Eqs. (5.2) and (5.3).

With combined information including the one gained in Sec. 5.2, i.e., $\mathbf{p}(x)=[0.3140,1]$, $\mathbf{p}(y_1|x)=[0.1526,0.6121]$, $\mathbf{p}(y_2|x)=[0.5412,1]$, $\mathbf{p}(y_1|x^C)=[0,1]$, $\mathbf{p}(y_2|x^C)=[0,1]$, $\mathbf{p}(Y_i|y_i)=[0.8,0.9]$, and $\mathbf{p}(Y_i^C|y_i^C)=[0.8,0.9]$ for $i=1,2$ and based on Theorem 5.3, we can find $\mathbf{p}(x|Y_1,Y_2)=[0.6364,1]$.

Compared with the single-point observation in Sec. 5.2, the epistemic uncertainty level is reduced faster with more information of observation used to assess the small scale property. This multipoint observation is an enhancement of the single-point observation and provides more information.

5.5 Multipoint Multiscale Observation. As a further extension of the multipoint observation approach, the experimental measures can be conducted at two or more scales for data analysis.

THEOREM 5.4. *Given* $\mathbf{p}(y_1,\ldots,y_M|x_1,\ldots,x_L)$ for variables $x_1,\ldots,x_L$ at scale X and $y_1,\ldots,y_M$ at scale Y, $\mathbf{p}(z_1,\ldots,z_N|y_1,\ldots,y_M)$ for variables $y_1,\ldots,y_M$ at scale Y and $z_1,\ldots,z_N$ at scale Z, $\mathbf{p}(Y_1,\ldots,Y_M|y_1,\ldots,y_M)$ for observable Y_m corresponding to y_m $(m=1,\ldots,M)$, $\mathbf{p}(Z_1,\ldots,Z_N|z_1,\ldots,z_N)$ for observable Z_n corresponding to z_n $(n=1,\ldots,N)$, and the prior estimate $\mathbf{p}(x_1,\ldots,x_L)$, the posterior probability $\mathbf{p}(x_1,\ldots,x_L|Y_1,\ldots,Y_M,Z_1,\ldots,Z_N)$ is obtained as

$$\mathbf{p}(x_1,\ldots,x_L|Y_1,\ldots,Y_M,Z_1,\ldots,Z_N)=\frac{\mathbf{p}(x_1,\ldots,x_L)\int\cdots\int\left[\begin{array}{l}\mathbf{p}(Z_1,\ldots,Z_N|z_1,\ldots,z_N)\\ \mathbf{p}(Y_1,\ldots,Y_M|y_1,\ldots,y_M)\\ \mathbf{p}(z_1,\ldots,z_N|y_1,\ldots,y_M)\\ \mathbf{p}(y_1,\ldots,y_M|x_1,\ldots,x_L)\end{array}\right]dz_1\cdots dz_N dy_1\cdots dy_M}{\text{dual}\int\cdots\int\left[\begin{array}{l}\mathbf{p}(Z_1,\ldots,Z_N|z_1,\ldots,z_N)\\ \mathbf{p}(Y_1,\ldots,Y_M|y_1,\ldots,y_M)\\ \mathbf{p}(z_1,\ldots,z_N|y_1,\ldots,y_M)\\ \mathbf{p}(y_1,\ldots,y_M|x_1,\ldots,x_L)\\ \mathbf{p}(x_1,\ldots,x_L)\end{array}\right]dz_1\cdots dz_N dy_1\cdots dy_M dx_1\cdots dx_L}$$

5.6 An Example of Multipoint Multiscale Observation. In the design of actuator in Fig. 3, a bending strain rate (M^2/mV^2) is used as one of the major metrics to measure the extent of bending movement for an actuator with respect to the squared electric field intensity. With the data in Ref. [50] and following the same procedure used in Secs. 5.2 and 5.4, we have

Downloaded 01 Mar 2011 to 130.207.50.192. Redistribution subject to ASME license or copyright; see http://www.asme.org/terms/Terms_Use.cfm

$$P(\text{bending\_strain\_rate} < 0.06 | \text{conductivity with 1\%CNT} < 0.1) = \mathbf{p}(z|y_1) = [0.2924, 1.0]$$

and

$$P(\text{bending\_strain\_rate} < 0.06 | \text{conductivity with 2\%CNT} < 0.1) = \mathbf{p}(z|y_2) = [0.3761, 1.0]$$

With $\mathbf{p}(x)=[0.3140,1]$, $\mathbf{p}(y_1|x)=[0.1526,0.6121]$, $\mathbf{p}(y_2|x)=[0.5412,1]$, $\mathbf{p}(y_1|x^C)=[0,1]$, $\mathbf{p}(y_2|x^C)=[0,1]$, $\mathbf{p}(z|y_1)=[0.2924,1.0]$, $\mathbf{p}(z|y_2)=[0.3761,1.0]$, $\mathbf{p}(z|y_1^C)=[0,1]$, $\mathbf{p}(z|y_2^C)=[0,1]$, $\mathbf{p}(Y_i|y_i)=[0.8,0.9]$, and $\mathbf{p}(Y_i^C|y_i^C)=[0.8,0.9]$ for $i=1,2$, $\mathbf{p}(Z|z)=[0.8,0.9]$, $\mathbf{p}(Z^C|z^C)=[0.8,0.9]$, and based on Theorem 5.4, we can find $\mathbf{p}(x|Y_1,Y_2,Z)=[0.57,1.0]$. Compared with the multipoint observation in Sec. 5.4, the epistemic uncertainty level is increased, which indicates that inconsistency in observations exists.

6 Concluding Remarks

The proposed GHMM is to represent aleatory and epistemic uncertainties simultaneously in analyzing multiscale systems, which is unavailable in existing multiscale uncertainty quantification methods. It captures coupling and dependency relationships between variables across different length scales in a generic way. The GHMM supports both parametric and nonparametric models of distributions. When the size or quality of data is not good enough to build parametric models, the nonparametric approach can be used without the assumption of distribution types.

The GHMM is based on a new theory of imprecise probability that has the form of generalized interval, where proper and improper intervals capture epistemic uncertainty in addition to probabilistic distributions for aleatory uncertainty. No assumptions of precise probability models and distribution types are required in imprecise probability if there is limited or no knowledge available. With an algebraic structure similar to the precise probability, the new generalized interval probability significantly simplifies the inference and reasoning compared with other forms of imprecise probabilities. The precise probability becomes a special case of the generalized interval probability, where the widths of interval probabilities are reduced to zeros. The proposed GHMM allows us to compute the propagation of uncertainties across length scales efficiently. Cross-scale information assimilation is enabled by a new definition of generalized interval Bayes' rule.

The proposed model and inference mechanisms help quantify multiscale uncertainty in system design and analysis. The simplicity of the reasoning based on the proposed model shows the advantages and potentials for a wide variety of applications. However, further investigation of fundamental properties of the generalized interval probability and GIBR is required in order to understand the completeness and soundness of interval estimations with respect to epistemic uncertainty. One limitation of the GIBR is that the completeness of the posterior probability cannot be checked directly by logic interpretation. In Eq. (5.1), $\mathbf{p}(A|E_i)$ and $\mathbf{p}(E_i)$ appear twice (the original and its dual respectively). One associated interpretation is $\forall$, and the other is $\exists$. The concatenation of the two predicates will be always $\exists$. As a result, the completeness of the epistemic component of $\mathbf{p}(E_i|A)$ cannot be checked directly, even though soundness can be done efficiently [37]. Therefore, some algorithmic approaches are required.

Acknowledgment

The author is thankful to Professor Wei Chen and Professor Chris Paredis for discussions, as well as anonymous reviewers.

Appendix A: Proof of Theorem 3.1

Proof.

$$\mathbf{p}(A \cap B|C) = \mathbf{p}(A|C)\mathbf{p}(B|C) \Leftrightarrow \mathbf{p}(A \cap B \cap C)/\text{dual}\mathbf{p}(C) = \mathbf{p}(A|C) \cdot \mathbf{p}(B \cap C)/\text{dual}\mathbf{p}(C) \Leftrightarrow \mathbf{p}(A \cap B \cap C)/\text{dual}\mathbf{p}(B \cap C)$$
$$= \mathbf{p}(A|C) \Leftrightarrow \mathbf{p}(A|B \cap C) = \mathbf{p}(A|C).$$

□

Appendix B: Proof of Theorem 4.1

Proof. By the definitions of conditional probability in Eq. (3.1) and independence in Eq. (3.3), we have

$$\mathbf{p}(X_{\mathcal{A}_i}, X_{\mathcal{A}_j}|x_{i\in\mathcal{A}_i}, x_{j\in\mathcal{A}_j}) = \frac{\mathbf{p}(X_{\mathcal{A}_i}, X_{\mathcal{A}_j}, x_{i\in\mathcal{A}_i}, x_{j\in\mathcal{A}_j})}{\text{dual}\mathbf{p}(x_{i\in\mathcal{A}_i}, x_{j\in\mathcal{A}_j})} = \frac{\mathbf{p}(X_{\mathcal{A}_i}, x_{i\in\mathcal{A}_i})\mathbf{p}(X_{\mathcal{A}_j}, x_{j\in\mathcal{A}_j})}{\text{dual}[\mathbf{p}(x_{i\in\mathcal{A}_i})\mathbf{p}(x_{j\in\mathcal{A}_j})]}$$
$$= \frac{\mathbf{p}(X_{\mathcal{A}_i}, x_{i\in\mathcal{A}_i})\mathbf{p}(X_{\mathcal{A}_j}, x_{j\in\mathcal{A}_j})}{\text{dual}\mathbf{p}(x_{i\in\mathcal{A}_i})\text{dual}\mathbf{p}(x_{j\in\mathcal{A}_j})} = \mathbf{p}(X_{\mathcal{A}_i}|x_{i\in\mathcal{A}_i})\mathbf{p}(X_{\mathcal{A}_j}|x_{j\in\mathcal{A}_j})$$

□

Appendix C: Proof of Theorem 4.2

Proof. By the definitions of conditional probability and independence, we have

$$\mathbf{p}(x_{\mathcal{A}_i}|y_{\mathcal{B}_j}, z_{\mathcal{C}_k}) = \frac{\mathbf{p}(x_{\mathcal{A}_i}, y_{\mathcal{B}_j}, z_{\mathcal{C}_k})}{\text{dual}\mathbf{p}(y_{\mathcal{B}_j}, z_{\mathcal{C}_k})} = \frac{\mathbf{p}(x_{\mathcal{A}_i}, y_{\mathcal{B}_j})\mathbf{p}(z_{\mathcal{C}_k})}{\text{dual}\mathbf{p}(y_{\mathcal{B}_j})\text{dual}\mathbf{p}(z_{\mathcal{C}_k})} = \mathbf{p}(x_{\mathcal{A}_i}|y_{\mathcal{B}_j})$$

since $\mathbf{p}(z_{\mathcal{C}_k})/\text{dual}\mathbf{p}(z_{\mathcal{C}_k})=1$. Similarly we derive $\mathbf{p}(z_{C_k}|y_{B_j}, x_{A_i}) = \mathbf{p}(z_{C_k}|y_{B_j})$. □

Appendix D: Proof of Theorem 5.1

Proof.

$$\frac{\mathbf{p}(A|E_i)\mathbf{p}(E_i)}{\sum_{j=1}^{n}\text{dual}\mathbf{p}(A|E_j)\text{dual}\mathbf{p}(E_j)} = \frac{\mathbf{p}(A|E_i)\mathbf{p}(E_i)}{\text{dual}\sum_{j=1}^{n}\mathbf{p}(A|E_j)\mathbf{p}(E_j)} = \frac{\mathbf{p}(A \cap E_i)}{\text{dual}\sum_{j=1}^{n}\mathbf{p}(A \cap E_j)} = \frac{\mathbf{p}(A \cap E_i)}{\text{dual}\mathbf{p}(A)}$$
$$= \mathbf{p}(E_i|A)$$

□

Downloaded 01 Mar 2011 to 130.207.50.192. Redistribution subject to ASME license or copyright; see http://www.asme.org/terms/Terms_Use.cfm

Appendix E: Proof of Theorem 5.2

Proof.

$$\mathbf{p}(x_1,\ldots,x_L|Y)=\frac{\mathbf{p}(Y,x_1,\ldots,x_L)}{\text{dual}\mathbf{p}(Y)}=\frac{\int(Y,y,x_1,\ldots,x_L)dy}{\text{dual}\mathbf{p}(Y)}$$

because of the logic coherent constraint $\int\mathbf{p}(y)dy=1$.

$$\frac{\int\mathbf{p}(Y,y,x_1,\ldots,x_L)dy}{\text{dual}\mathbf{p}(Y)}=\frac{\mathbf{p}(x_1,\ldots,x_L)\int\mathbf{p}(Y|y)\mathbf{p}(y|x_1,\ldots,x_L)dy}{\text{dual}\int\cdots\iint\mathbf{p}(Y|y)\mathbf{p}(y|x_1,\ldots,x_L)\mathbf{p}(x_1,\ldots,x_L)dydx_1\cdots dx_L}$$

because of Theorem 3.1. □

Appendix F: Proof of Theorem 5.3

Proof.

$$\mathbf{p}(x_1,\ldots,x_L|Y_1,\ldots,Y_M)=\frac{\mathbf{p}(Y_1,\ldots,Y_M,x_1,\ldots,x_L)}{\text{dual}\mathbf{p}(Y_1,\ldots,Y_M)}=\frac{\int\cdots\int\mathbf{p}(Y_1,\ldots,Y_M,y_1,\ldots,y_M,x_1,\ldots,x_L)dy_1\cdots dy_M}{\text{dual}\int\cdots\int\mathbf{p}(Y_1,\ldots,Y_M,y_1,\ldots,y_M,x_1,\ldots,x_L)dy_1\cdots dy_Mdx_1\cdots dx_L}$$

$$=\frac{\int\cdots\int\begin{bmatrix}\mathbf{p}(Y_1,\ldots,Y_M|y_1,\ldots,y_M)\\\times\mathbf{p}(y_1,\ldots,y_M|x_1,\ldots,x_L)\\\times\mathbf{p}(x_1,\ldots,x_L)\end{bmatrix}dy_1\cdots dy_M}{\text{dual}\int\cdots\int\begin{bmatrix}\mathbf{p}(Y_1,\ldots,Y_M|y_1,\ldots,y_M)\\\times\mathbf{p}(y_1,\ldots,y_M|x_1,\ldots,x_L)\\\times\mathbf{p}(x_1,\ldots,x_L)\end{bmatrix}dy_1\cdots dy_Mdx_1\cdots dx_L}$$

because of Theorem 3.1. If $y_1,\ldots,y_M$ and their measurements $Y_1,\ldots,Y_M$ are mutually independent, from Theorem 4.1, the above can be simplified further to

$$\mathbf{p}(x_1,\ldots,x_L|Y_1,\ldots,Y_M)=\frac{\mathbf{p}(x_1,\ldots,x_L)\int\cdots\int\begin{bmatrix}\prod_{m=1}^{M}\mathbf{p}(Y_m|y_m)\\\times\prod_{m=1}^{M}\mathbf{p}(y_m|x_1,\ldots,x_L)\end{bmatrix}dy_1\cdots dy_M}{\text{dual}\int\cdots\int\begin{bmatrix}\prod_{m=1}^{M}\mathbf{p}(Y_m|y_m)\\\times\prod_{m=1}^{M}\mathbf{p}(y_m|x_1,\ldots,x_L)\\\times\mathbf{p}(x_1,\ldots,x_L)\end{bmatrix}dy_1\cdots dy_Mdx_1\cdots dx_L}$$

□

Appendix G: Proof of Theorem 5.4

Proof of Theorem 5.4 is similar to the proof of Theorem 5.3.

References

[1] Walley, P., 1991, *Statistical Reasoning With Imprecise Probabilities*, Chapman & Hall, London.

[2] Oberkampf, W. L., DeLand, S. M., Rutherford, B. M., Diegert, K. V., and Alvin, K. F., 2002, "Error and Uncertainty in Modeling and Simulation," Reliab. Eng. Syst. Saf., **75**(3), pp. 333–357.

[3] Klir, G. J., 2006, *Uncertainty and Information: Foundation of Generalized Information Theory*, Wiley, New York.

[4] Campolongo, F., Saltelli, A., and Tarantola, S., 2000, "Sensitivity Analysis as an Ingredient of Modeling," Stat. Sci., **15**(4), pp. 377–395.

[5] Hoffman, F. O., and Hammonds, J. S., 1994, "Propagation of Uncertainty in Risk Assessments: The Need to Distinguish Between Uncertainty Due to Lack of Knowledge and Uncertainty Due to Variability," Risk Anal., **14**(5), pp. 707–712.

[6] Elishakoff, I., and Ren, Y., 2003, *Finite Element Methods for Structures With Large Stochastic Variations*, Oxford University Press, Oxford.

[7] Liu, W. K., Belytschko, T., and Mani, A., 1986, "Random Field Finite Elements," Int. J. Numer. Methods Eng., **23**(10), pp. 1831–1845.

[8] Ghanem, R. G., and Spanos, P. D., 2003, *Stochastic Finite Elements: A Spectral Approach*, Springer-Verlag, New York.

[9] Xiu, D., and Karniadakis, G. E., 2003, "Modeling Uncertainty in Flow Simulations via Generalized Polynomial Chaos," J. Comput. Phys., **187**(1), pp. 137–167.

[10] Xiu, D., and Hesthaven, J. S., 2005, "High-Order Collocation Methods for Differential Equations With Random Inputs," SIAM (Soc. Ind. Appl. Math.) J. Sci. Stat. Comput., **27**(3), pp. 1118–1139.

[11] Babuška, I., Nobile, F., and Tmpone, R., 2007, "A Stochastic Collocation Method for Elliptic Partial Differential Equations With Random Input Data," SIAM (Soc. Ind. Appl. Math.) J. Numer. Anal., **45**(3), pp. 1005–1034.

[12] Sudret, B., and Der Kiureghian, A., 2000, "Stochastic Finite Element Methods and Reliability—A State-of-the-Art Report," University of California Berkeley Report No. UCB/SEMM-2000/08.

[13] Kubin, L.P., Canova, G., Condat, M., Devincre, B., Pontikis, V., and Bréchet Y., 1992, "Dislocation Microstructures in Two Dimensions: I. Relaxed Struc-

Downloaded 01 Mar 2011 to 130.207.50.192. Redistribution subject to ASME license or copyright; see http://www.asme.org/terms/Terms_Use.cfm

tures, Modeling Simulation," Solid State Phenom., **23–24**, pp. 455–472.
[14] Hähner, P., 1996, "A Theory of Dislocation Cell Formation Based on Stochastic Dislocation Dynamics," Acta Mater., **44**(6), pp. 2345–2352.
[15] El-Azab, A., 2000, "Statistical Mechanics Treatment of the Evolution of Dislocation Distributions in Single Crystals," Phys. Rev. B, **61**(18), pp. 11956–11966.
[16] Zaiser, M., 2001, "Statistical Modeling of Dislocation Systems," Mater. Sci. Eng., A, **309–310**, pp. 304–315.
[17] Hiratani, M., and Zbib, H. M., 2003, "On Dislocation-Defect Interactions and Patterning: Stochastic Discrete Dislocation Dynamics (SDD)," J. Nucl. Mater., **323**(2–3), pp. 290–303.
[18] Liu, W. K., Siad, L., Tian, R., Lee, S., Lee, D., Yin, X., Chen, W., Chan, S., Olson, G. B., Lindgen, L.-E., Horstemeyer, M. F., Chang, Y.-S., Choi, J.-B., and Kim, Y. J., 2009, "Complexity Science of Multiscale Materials via Stochastic Computations," Int. J. Numer. Methods Eng., **80**(6–7), pp. 932–978.
[19] Choi, M. J., Chandrasekaran, V., Malioutov, D. M., Johnson, J. K., and Willsky, A. S., 2008, "Multiscale Stochastic Modeling for Tractable Inference and Data Assimilation," Comput. Methods Appl. Mech. Eng., **197**(43–44), pp. 3492–3515.
[20] Chamoin, L., Oden, J. T., and Prudhomme, S., 2008, "A Stochastic Coupling Method for Atomic-to-Continuum Monte-Carlo Simulations," Comput. Methods Appl. Mech. Eng., **197**(43–44), pp. 3530–3546.
[21] Ganapathysubramanian, B., and Zabaras, N., 2008, "Modeling Multiscale Diffusion Processes in Random Heterogeneous Media," Comput. Methods Appl. Mech. Eng., **197**(43–44), pp. 3560–3573.
[22] Arnst, M., and Ghanem, R., 2008, "Probabilistic Equivalence and Stochastic Model Reduction in Multiscale Analysis," Comput. Methods Appl. Mech. Eng., **197**(43–44), pp. 3584–3592.
[23] Yin, X., Lee, S., Chen, W., Liu, W. K., and Horstemeyer, M. F., 2009, "Efficient Random Field Uncertainty Propagation in Design Using Multiscale Analysis," ASME J. Mech. Des., **131**(2), p. 021006.
[24] Chen, W., Yin, X., Lee, S., and Liu, W. K., 2010, "A Multiscale Design Methodology for Hierarchical Systems With Random Field Uncertainty," ASME J. Mech. Des., **132**(4), p. 041006.
[25] van Fraassen, B., 1989, *Laws and Symmetry*, Clarendon, Oxford.
[26] Dempster, A., 1967, "Upper and Lower Probabilities Induced by a Multi-Valued Mapping," Ann. Math. Stat., **38**(2), pp. 325–339.
[27] Shafer, G. A., 1990, *Mathematical Theory of Evidence*, Princeton University Press, Princeton, NJ.
[28] Williams, P. M., 2007, "Notes on Conditional Previsions," Int. J. Approx. Reason., **44**, pp. 366–383.
[29] Dubois, D., and Prade, H., 1988, *Possibility Theory: An Approach to Computerized Processing of Uncertainty*, Plenum, New York.
[30] Ferson, S., Kreinovich, V., Ginzburg, L., Myers, D. S., and Sentz, K., 2003, "Constructing Probability Boxes and Dempster-Shafer Structures," Sandia National Laboratories Technical Report No. SAND2002-4015.
[31] Weichselberger, K., 2000, "The Theory of Interval-Probability as a Unifying Concept for Uncertainty," Int. J. Approx. Reason., **24**(2–3), pp. 149–170.
[32] Molchanov, I., 2005, *Theory of Random Sets*, Springer, London.
[33] Kuznetsov, V. P., 1995, "Interval Methods for Processing Statistical Characteristics," Proceedings of the 1995 International Workshop on Applications of Interval Computations, El Paso, TX.
[34] Möller, B., and Beer, M., 2004, *Fuzzy Randomness: Uncertainty in Civil Engineering and Computational Mechanics*, Springer, Berlin.
[35] Neumaier, A., 2004, "Clouds, Fuzzy Sets, and Probability Intervals," Reliab. Comput., **10**(4), pp. 249–272.
[36] Wang, Y., 2008, "Imprecise Probabilities With a Generalized Interval Form," Proceedings of the Third Workshop on Reliability Engineering Computing (REC'08), Savannah, GA, pp. 45–59.
[37] Wang, Y., 2010, "Imprecise Probabilities Based on Generalized Intervals for System Reliability Assessment," International Journal of Reliability & Safety, **4**(4), pp. 319–342.
[38] Kaucher, E., 1980, "Interval Analysis in the Extended Interval Space IR," *Computing Supplementa*, Suppl. 2, Springer-Verlag, New York, pp. 33–49.
[39] Gardeñes, E., Sainz, M. Á., Jorba, L., Calm, R., Estela, R., Mielgo, H., and Trepat, A., 2001, "Modal Intervals," Reliab. Comput., **7**(2), pp. 77–111.
[40] Dimitrova, N. S., Markov, S. M., and Popova, E. D., 1992, "Extended Interval Arithmetics: New Results and Applications," *Computer Arithmetic and Enclosure Methods*, L. Atanassova and J. Herzberger, eds., pp. 225–232.
[41] Moore, R. E., 1966, *Interval Analysis*, Prentice-Hall, Englewood Cliffs, NJ.
[42] Wang, Y., 2008, "Semantic Tolerance Modeling With Generalized Intervals," ASME J. Mech. Des., **130**(8), p. 081701.
[43] Wang, Y., 2008, "Closed-Loop Analysis in Semantic Tolerance Modeling," ASME J. Mech. Des., **130**(6), p. 061701.
[44] Wang, Y., 2008, "Interpretable Interval Constraint Solvers in Semantic Tolerance Analysis," Comput.-Aided Des., **5**(5), pp. 654–666.
[45] MacDonald, I. L., and Zucchini, W., 1997, *Hidden Markov and Other Models for Discrete-Valued Time Series*, Chapman and Hall, London/CRC, Boca Raton, FL.
[46] Cappé, O., Moulines, E., and Rydén, T., 2005, *Inference in Hidden Markov Models*, Springer, New York.
[47] Fine, S., Singer, Y., and Tishby, N., 1998, "The Hierarchical Hidden Markov Model: Analysis and Applications," Mach. Learn., **32**, pp. 41–62.
[48] Bouman, C. A., and Shapiro, M., 1994, "A Multiscale Random Field Model for Bayesian Image Segmentation," IEEE Trans. Image Process., **3**(2), pp. 162–177.
[49] Laferté, J. M., Perez, P., and Heitz, F., 2000, "Discrete Markov Modeling and Inference on the Quad-Tree," IEEE Trans. Image Process., **9**(3), pp. 390–404.
[50] Deshmukh, S., and Ounaies, Z., 2009, "Single Walled Carbon Nanotube (SWNT)-Polymide Nanocomposites as Electrostrictive Materials," Sens. Actuators, A, **155**(2), pp. 246–252.
[51] Dai, H., Wong, E. W., and Lieber, C. M., 1996, "Probing Electrical Transport in Nanomaterials: Conductivity of Individual Carbon Nanotubes," Science, **272**(5261), pp. 523–526.
[52] Ebbesen, T. W., Lezec, H. J., Hiura, H., Bennett, J. W., Ghaemi, H. F., and Thio, T., 1996, "Electrical Conductivity of Individual Carbon Nanotubes," Nature (London), **382**, pp. 54–56.
[53] Bauhofer, W., and Kovacs, J. Z., 2009, "A Review and Analysis of Electrical Percolation in Carbon Nanotube Polymer Composites," Compos. Sci. Technol., **69**(10), pp. 1486–1498.

Downloaded 01 Mar 2011 to 130.207.50.192. Redistribution subject to ASME license or copyright; see http://www.asme.org/terms/Terms_Use.cfm